Chemical Engineering Journal 375 (2019) 121916

Contents lists available at ScienceDirect

Chemical Engineering Journal

journal homepage: www.elsevier.com/locate/cej

A novel phosphorus/nitrogen-containing polycarboxylic acid endowing epoxy resin with excellent flame retardance and mechanical properties

Huajun Duan[a], Yongsheng Chen[a], Sa Ji[a], Rui Hu[a], Huiru Ma[b,*]

[a] School of Materials Science and Engineering, Wuhan University of Technology, 122 Luoshi Road, Wuhan 430070, China
[b] Department of Chemistry, School of Chemistry, Chemical Engineering and Life Science, Wuhan University of Technology, 122 Luoshi Road, Wuhan 430070, China

HIGHLIGHTS

- A novel polycarboxylic acid containing DOPO and triazine-trione was synthesized.
- TMD significantly improves the fire safety of EP.
- TMD slightly enhances the mechanical properties of EP.
- The cured EP maintains its thermostability and transparency.

GRAPHICAL ABSTRACT

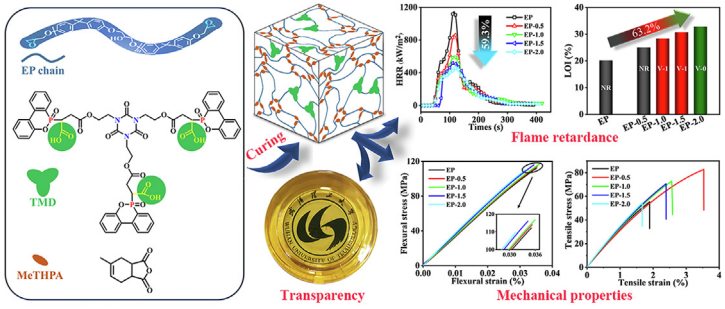

ARTICLE INFO

Keywords:
Polycarboxylic acid
Epoxy resin
Flame retardance
Mechanical properties

ABSTRACT

To meet the requirements of application of epoxy resin (EP) in some special fields, the flame retardance must be improved without losing its mechanical properties. To achieve this purpose, a novel phosphorus/nitrogen-containing polycarboxylic acid (TMD) was synthesized successfully via a facile monoesterification and addition reaction between 1,3,5-tris(2-hydroxyethyl)isocyanurate (THEIC), maleic anhydride (MAH) and 9,10-dihydro-9-oxa-10-phosphaphenanthrene-10-oxide (DOPO), and used as reactive flame retardant for anhydride-cured epoxy system. The structure of TMD was confirmed by Fourier transform infrared (FTIR) spectra and nuclear magnetic resonance (NMR). Thermogravimetric analysis (TGA) indicated that after the introduction of TMD, cured EP maintained good thermal stability owing to the cross-linking reaction of TMD and EP. Besides, with the addition of 26.0 wt% TMD (2.0 wt% phosphorous loading), the limited oxygen index (LOI) value of cured EP increased from 20.1% of pure EP to 32.8%, and vertical burning (UL-94) V-0 rating was achieved. Compared with pure EP, its peak heat release rate (PHRR) sharply decreased by 59.3% in the cone calorimeter (CC) test. All those results suggested that TMD endowed EP with excellent flame retardance. The investigations on char residue of cured EP and pyrolysis process of TMD further revealed that TMD exerted bi-phase flame-retardant effects. Additionally, because of the formation of heterogeneous network and hydrogen bonds, cured EP possessed good mechanical properties including tensile modulus and strength as well as flexural modulus and strength. Meantime, it presented great transparency due to the excellent compatibility of TMD with EP.

* Corresponding author.
E-mail address: mahr@whut.edu.cn (H. Ma).

https://doi.org/10.1016/j.cej.2019.121916
Received 11 March 2019; Received in revised form 24 May 2019; Accepted 7 June 2019
Available online 10 June 2019
1385-8947/

1. Introduction

Epoxy resin (EP), considered as a significant thermosetting polymer, has been extensively employed in various areas such as aerospace, coatings, adhesives, electronic devices, laminates and encapsulations due to the characteristics of outstanding mechanical and electrical properties, relatively low curing shrinkage, superior adhesion to substrates as well as good thermal, chemical and corrosion resistance [1–6]. However, the flammability of EP extremely restricts its further applications, especially in some fields with high flame-retardant requirements [7,8].

To endow EP with expected flame retardance, different flame-retardant elements such as halogen [9,10], phosphorus [11,12], nitrogen [13,14], boron [15,16] and silicon [17,18] were introduced into EP. In despite of possessing high flame-retardant efficiency and little influence on comprehensive properties of EP, halogen-containing flame retardants have been gradually restrained in recent years owing to their producing poisonous and corrosive substances during combustion which are harmful to the natural ecosystem and human health [19,20]. Therefore, halogen-free flame retardants, particularly phosphorus-containing ones have gradually drawn more and more attention because of their strong ability of capturing free radical to interrupt the burning reactions in gas phase and excellent effect of charring to block heat and oxygen exchange in condensed phase [21,22]. Besides, when flame-retardant systems simultaneously contain phosphorus and nitrogen elements, flame-retardant efficiency can be further improved, where P-containing parts promote charring as the dehydrating agent in condensed phase, while N-containing parts make main contribution in gas phase [23].

In recent years, because of the high reactivity, thermal stability and flame-retardant efficiency, the phosphorus-containing compounds, 9,10-dihydro-9-oxa-10-phosphaphenanthrene-10-oxide (DOPO) and its derivatives have been widely used in flame-retardant EP [24–26]. Furthermore, the applications of triazine-based compounds such as ammonium polyphosphate (APP) and melamine cyanurate (MCA) in flame-retardant polymers have been frequently reported due to their excellent flame retardance by releasing inert gas and promoting the charring effect [27,28]. In view of the aforementioned facts, many researchers have synthesized flame retardants containing these two chemical structures and imparted great flame retardance to EP, and also demonstrated the synergistic effect between those two flame-retardant groups. L. Qian et al. [29] modified the 1,3,5-triglycidyl isocyanurate (TGIC) with DOPO through a controllable ring-opening addition reaction to obtain efficient flame retardant TGIC-DOPO. The results indicated that the EP with 12 wt% TGIC-DOPO content achieved vertical burning (UL-94) V-0 rating, and the limited oxygen index (LOI) value increased from 22.5% of pure EP to 33.3%. In the study of S. Huo et al. [30], a novel flame retardant DMT containing phosphaphenanthrene, maleimide and triazine-trione groups was successfully synthesized. With only 1.0 wt% phosphorus content loading, the cured EP acquired a high LOI value of 35.8% and passed UL-94V-0 rating. However, most of them are additive flame retardants which are only physically blended in epoxy. Generally, the high loadings of flame retardants and poor compatibility with EP will deteriorate the mechanical properties of EP. In addition, these additive flame retardants will gradually leach from matrix, resulting in the degradation of flame retardance and environmental pollution [31]. In contrast, the reactive flame retardants, chemically connected to the crosslinking network of EP, can endow EP with sustainable fire resistance and finally cured EP exhibits satisfactory physical and mechanical properties.

Additionally, the researches on flame retardance of EP mostly used amine curing agent because that the existence of nitrogen in amine curing agent makes a contribution to flame retardance of EP. However, it is well known that anhydride-cured epoxy always possesses better comprehensive properties than amine-cured epoxy such as a lower initial viscosity, longer pot life, lower water absorption, great transparency and especially outstanding dielectric properties [32–34]. Therefore, the use of anhydride-cured epoxy is very common in electrical/electronic fields such as electronic insulation sealants for integrated circuits and semiconductor-based electronic systems [35,36]. It should be mentioned that as the electronic devices develop in a highly integrated direction in recent years, overheating of electronic devices has become more serious, which is more likely to cause fire hazards [37]. Therefore, the research on flame retardance of the anhydride-cured epoxy resin system seems particularly significant.

In this paper, a novel reactive flame retardant TMD containing phosphaphenanthrene and triazine-trione groups was prepared via a facile monoesterification and addition reaction between 1,3,5-tris(2-hydroxyethyl)isocyanurate (THEIC), maleic anhydride (MAH) and DOPO. After the incorporation of the TMD into EP and being cured by methyltetrahydrophthalic anhydride (MeTHPA), the obtained flame-retardant EP (FREP) simultaneously possessed excellent flame retardance and good mechanical properties as well as great transparency. Furthermore, the synthesis of TMD utilized the low-cost and nontoxic industrial raw materials, meanwhile there were no corrosive gases or toxic substances producing in the reaction process, which meets environmental requirements. All these suggest it has numerous industrialized potential uses in the electrical/electronic fields. The chemical structure of TMD and the comprehensive performances of cured EP including curing behavior, transparency, thermal stability, flame retardance, combustion behavior and mechanical properties have been investigated in detail.

2. Experimental section

2.1. Materials

Epoxy resin (E-51, the epoxy value of 0.51 mol/100 g) was purchased from Yueyang Baling Huaxing Petrochemical Co., Ltd. 9,10-Dihydro-9-oxa-10-phosphaphenanthrene-10-oxide (DOPO) was provided by Huizhou Shengshi Technology Co. Ltd. 1,3,5-tris(2-hydroxyethyl)isocyanurate (THEIC) was obtained from Guangdong Wengjiang Chemical Reagent Co., Ltd. Maleic anhydride (MAH) was provided by Tianjin Beilian Fine Chemicals Development Co., Ltd. 1,4-Dioxane was purchased from Sinopharm Chemical Reagent Co., Ltd. Methyltetrahydrophthalic anhydride (MeTHPA) was provided by Wuhan Hanhai Synthetic Resin Development Co., Ltd. 2,4,6-Tris(dimethylaminomethyl)phenol (DMP-30) was purchased from Sinopharm Chemical Reagent Co., Ltd. All reagents were used as received.

2.2. Synthesis of TMD

THEIC (78.3 g, 0.3 mol), MAH (88.2 g, 0.9 mol) and dioxane (80 mL) were successively introduced into a 500 mL three-necked round-bottom glass flask equipped with a mechanical stirrer, reflux condenser and thermometer. The reaction mixture was heated to 95 °C and maintained at that temperature for 2 h with constant stirring. After that, DOPO (194.4 g, 0.9 mol) and dioxane (120 mL) were added in batches within 30 min. The solution was further heated to reflux for 8 h. Thereafter, the resultant solution was poured into deionized water and the white viscous product was obtained after being filtered. The crude product was washed by excessive deionized water, and then vacuum-dried at 80 °C for 24 h to a constant weight. The corresponding synthetic route of TMD was shown in Scheme 1. Yield: 90.1%. The chemical structure of TMD was confirmed by FTIR, ^{1}H NMR and ^{31}P NMR. FTIR (KBr, cm^{-1}): 3431 (COOH), 3070 (Ar-H), 2885–2905 (C–H), 1740 and 1693 (C=O), 1596 (C_6H_6), 1366 (C-N), 1200 (P=O), and 925 (P-O-C). ^{1}H NMR (400 MHz, DMSO-d_6, ppm): 13.10–12.65 (H^f), 8.36–7.19 (H^e), 4.34–4.02 (H^b), 3.79–3.43 (H^a), 3.00–2.57 (H^c), and 4.02–3.83 (H^d). ^{31}P NMR (400 MHz, DMSO-d_6, ppm): 29.8.

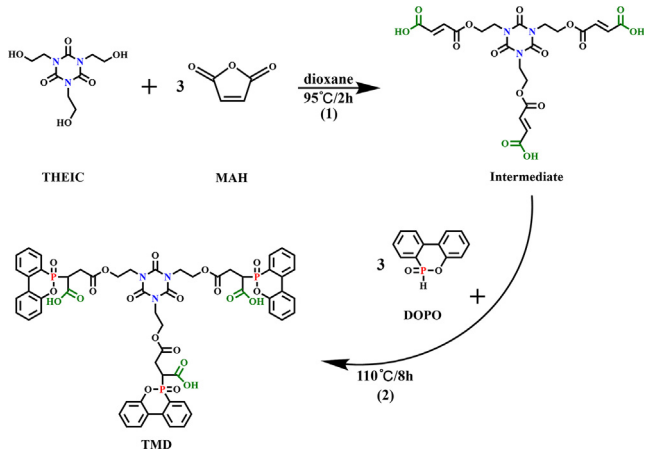

Scheme 1. Synthesis route of TMD.

2.3. Preparation of flame-retardant EP

EP and TMD were blended at 140 °C until a homogeneous solution was obtained. Then MeTHPA as curing agent and DMP-30 (0.2 wt% of epoxy resin) as curing accelerator were added into the solution sequentially after the solution was cooled to 75 °C. The mixture was stirred constantly and then deaerated under vacuum for 5 min. Thereafter, it was poured into a preheated mold and cured at 100 °C for 4 h and then at 130 °C for 2 h, 180 °C for 2 h, followed by a post-curing at 200 °C for another 2 h. Furthermore, the control samples including the pure EP and EP-DOPO systems were also prepared by the same procedure but respectively without the addition of TMD and with the addition of DOPO at 80 °C. The formulations of all samples were listed in Table 1. In all the systems of EP, the mole ratio of anhydride, carboxylic acid and DOPO to epoxy group was 1: 1.

2.4. Characterizations

Fourier transform infrared (FTIR) spectra were carried out on a Nicolet 6700 infrared spectrometer (Nicolet, America) over the wavenumber range of 4000 to 400 cm^{-1} using KBr pellets.

Nuclear magnetic resonance (NMR) was measured on a Bruker AV400 NMR spectrometer (Bruker, Switzerland) using deuterated dimethyl sulfoxide (DMSO-d_6) as the solvent.

Thermogravimetric analysis (TGA) was performed using STA449F3 (NETZSCH, Germany) at a heating rate of 10 °C/min within a temperature range from 40 °C to 800 °C under a nitrogen flow of 50 mL/min.

The limited oxygen index (LOI) values were measured on a JF-3 oxygen index meter (Jiangning, China) according to ASTM D2863 with a size of 100 × 6.5 × 3 mm^3.

Vertical burning (UL-94) tests were measured using NK8017A instrument (Nklsky, China) with the dimension of 130 × 13 × 3 mm^3 according to ASTM D3801. The results for each sample were obtained from at least five measurements.

Cone calorimeter (CC) tests were performed to analyze the combustion behavior of the samples with a FTT0007 cone calorimeter (FTT, Britain) according to the ISO 5660 standard under an external heat flux of 50 kW/m^2. The size of samples was 100 × 100 × 3 mm^3.

Differential scanning calorimetry (DSC) was measured with Perkin-Elmer DSC 4000 (PE, USA) at a heating rate of 5 °C/min under nitrogen atmosphere.

Dynamic mechanical analysis (DMA) was performed on Pyris Diamond dynamic thermal mechanical analyzer (PE, USA). The sample was tested in three-point bending pattern at a heating rate of 5 °C/min and constant frequency of 1 Hz. The dimension of sample for DMA test is 40 × 6 × 3 mm^3.

Scanning electronic microscopy (SEM, TESCAN VEGA3, Czech Republic) was applied to observe the surficial morphology of residue after cone calorimeter.

Laser raman spectroscopy (LRS) measurements were carried out at room temperature with an InVia laser Raman spectrometer (RENISHAW, Britain). The excitation wavelength was 633 nm and the scanning range was 2000 to 800 cm^{-1}.

Pyrolysis-gas chromatography/mass spectrometry (Py-GC/MS) was carried out with an Agilent 7890/5975 GC/MS (Agilent, USA). The injector temperature was 250 °C, 1 min at 50 °C then the temperature was increased to 280 °C at a rate of 8 °C/min. The temperature of the GC/MS interface was 280 °C, and the cracker temperature was 500 °C.

Tensile and flexural properties were analyzed at room temperature with a universal material testing machine (Instron 5967, USA). The dumbbell-shaped tensile samples were tested according to ASTM D638 at a speed of 1 mm/min. Flexural properties were performed in three-point bending mode according to ASTM D790. Each sample was tested for at least five times, and the averaged results were reported.

3. Results and discussion

3.1. Structure characterization of TMD

FTIR, ^1H NMR and ^{31}P NMR were used to characterize the chemical structure of TMD. The FTIR spectra of DOPO, MAH, THEIC and TMD were presented in Fig. 1. From the FTIR spectrum of TMD, it was observed that the stretching vibration absorption peaks of –OH derived from THEIC at 3490 cm^{-1}, 3373 cm^{-1} and 3256 cm^{-1} as well as the typical absorption peaks of C=O origin from anhydride at 1850 cm^{-1} and 1786 cm^{-1} disappeared, and a new peak at 3428 cm^{-1} which can be attributed to the characteristic absorption peak of -COOH appeared, demonstrating the monoesterification reaction of THEIC and MAH. Furthermore, the stretching vibration absorption peak of C=C at 1635 cm^{-1} and P-H at 2437 cm^{-1} respectively found in MAH and DOPO disappeared in the FTIR spectrum of TMD, which indicated that the addition reaction between intermediate and DOPO had completely occurred. In addition, in the FTIR spectrum of TMD, the absorption peaks at 1740 cm^{-1} and 1693 cm^{-1} can be ascribed to the stretching vibration of C=O, and the absorption peaks at 1366 cm^{-1}, 1200 cm^{-1} and 925 cm^{-1} can be respectively attributed to the stretching

Table 1
Formulations of cured epoxy.

Sample	DGEBA (g)	DMP-30 (g)	MeTHPA (g)	DOPO (g)	TMD		P content (wt%)
					(g)	(wt%)	
EP	100	0.2	84.7	0	0	0	0
EP-DOPO	100	0.2	64.2	26.8	0	0	2.0
EP-0.5	100	0.2	79.5	0	12.5	6.5	0.5
EP-1.0	100	0.2	73.9	0	26.0	13.0	1.0
EP-1.5	100	0.2	67.8	0	40.7	19.5	1.5
EP-2.0	100	0.2	61.2	0	56.6	26.0	2.0

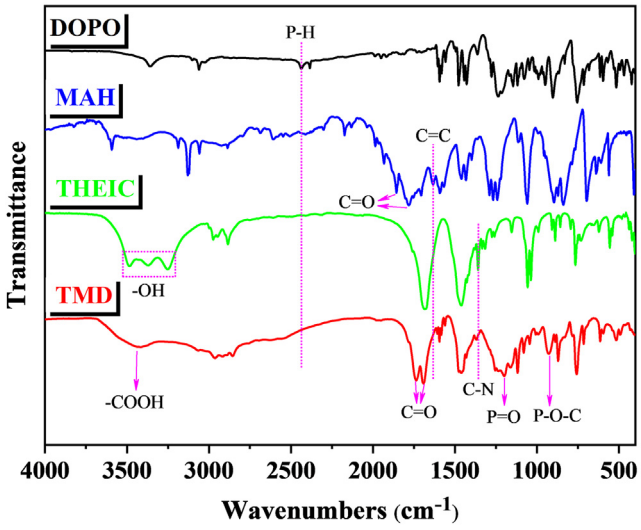

Fig. 1. FTIR spectra of DOPO, MAH, THEIC and TMD.

vibrations of C-N, P=O and P-O-C [30]. The information mentioned above indicated the existence of the phosphaphenanthrene and triazine-trione groups in the molecular structure of TMD.

The ^{1}H NMR and ^{31}P NMR spectra of TMD were shown in Fig. 2. As shown in Fig. 2a, it was found that there were six types of hydrogen. 13.10–12.65 ppm was assigned to the chemical shift of reactive hydrogen of carboxyl (COOH, H^{f}); 8.36–7.19 ppm was attributed to the chemical shift of aromatic hydrogen of DOPO group (Ar-H, H^{e}); 4.34–4.02 ppm, 3.79–3.43 ppm and 3.00–2.57 ppm corresponded to the chemical shift of CH_2 in CH_2-O (H^{b}), N-CH_2 (H^{a}) and O=C-CH_2 (H^{c}), respectively; 4.02–3.83 ppm can be regarded as the chemical shift of CH linked with DOPO group (DOPO-CH, H^{d}) [15,29]. Moreover, it was obvious that the ^{31}P NMR spectrum of TMD in Fig. 2b showed a single peak at 29.8 ppm, while the chemical shift of phosphorus atom in DOPO shown in Fig. 2c was at 17.4–12.8 ppm. These results further confirmed that TMD was synthesized successfully.

3.2. Curing behavior

The reactions of epoxy with anhydride and carboxylic acid under the catalysis of tertiary amine have been well explored in many literatures [38,39]. As illustrated in Scheme 2a, the tertiary amine reacts with the anhydride to form a carboxylate firstly. Then the carboxylate opens the oxirane ring and the formed alkoxide intermediate can react with anhydride to form a polyester. Likewise, in Scheme 2b, carboxylic acid reacts with tertiary amine to form carboxylate anion, which can open the oxirane ring and formed hydrocarbon oxygen anion reacts with carboxylic acid. Generated carboxylate anion circulates the above reaction process and finally forms a polyester. According to these two reaction mechanisms, the final crosslinking system of this study was depicted in Scheme 2c, where (1), (2) and (3) refer to the crosslinking segments of epoxy with MeTHPA, epoxy with TMD, epoxy with MeTHPA and TMD, respectively.

To investigate the influence of flame retardant on the curing behavior of EP, all samples were tested by DSC at a heating rate of 5 °C/min in nitrogen atmosphere. As shown in Fig. 3, both pure EP and FREP showed only one exothermic peak (T_p). Whereas, T_p gradually shifted to a higher temperature with the addition amount of TMD increasing, indicating a more difficult curing reaction. This phenomenon was caused by the fact that the reactive activity of carboxylic acid towards epoxy is lower than that of anhydride towards epoxy. Moreover, the steric hindrance of TMD containing DOPO and triazine-trione rigid groups will also lower the reactive activity of carboxylic acid towards EP.

Furthermore, the digital photos of cured EP and FREP were presented in Fig. 4. It was clear that all the samples showed high transparency, indicating the excellent compatibility of TMD with EP. This is rare in the related study of flame retardancy of EP. Therefore, it behaves great potential application value in some special fields such as multi-functional gradient coating, light-emitting diodes (LEDs) and arts [40].

3.3. Thermal stability of FREP

The thermal degradation behaviors of EP and FREP in nitrogen atmosphere were evaluated by TGA. The TGA and DTG curves were shown in Fig. 5a, b, and the corresponding data were summarized in Table 2, including the initial decomposition temperature ($T_{5\%}$), the maximum decomposition temperature (T_{max}), the maximum decomposition rate (R_{max}) and the char residue at 800 °C. As shown in Fig. 5b, all the samples exhibited a single decomposition process, occurring approximately from 350 °C to 500 °C. With the content of TMD increasing, $T_{5\%}$ of FREP had a tiny decrease (from 356.9 °C to 348.7 °C). Similarly, T_{max} of FREP shifted to a lower temperature (from 407.5 °C to 389.7 °C). The declinations of $T_{5\%}$ and T_{max} suggested the earlier degradation of FREP, which can be explained by the lower thermal stability of P-O-C group from TMD compared with the C–C bond [41]. However, the declination of $T_{5\%}$ was not obvious in contrast to many researches where the decrease of $T_{5\%}$ was approximately 40 °C [26,42], illustrating the little influence of TMD on the thermal stability of FREP.

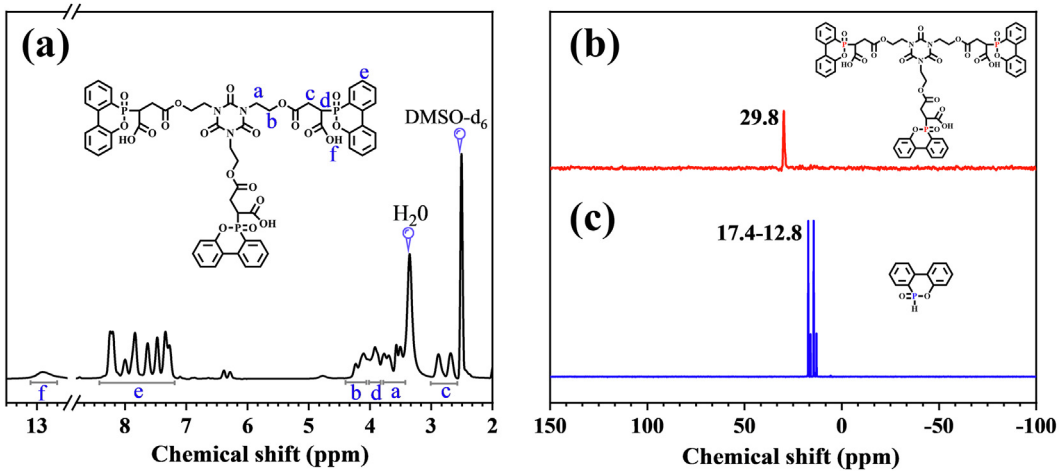

Fig. 2. ^{1}H NMR spectra of TMD (a) and ^{31}P NMR spectra of TMD (b) and DOPO (c).

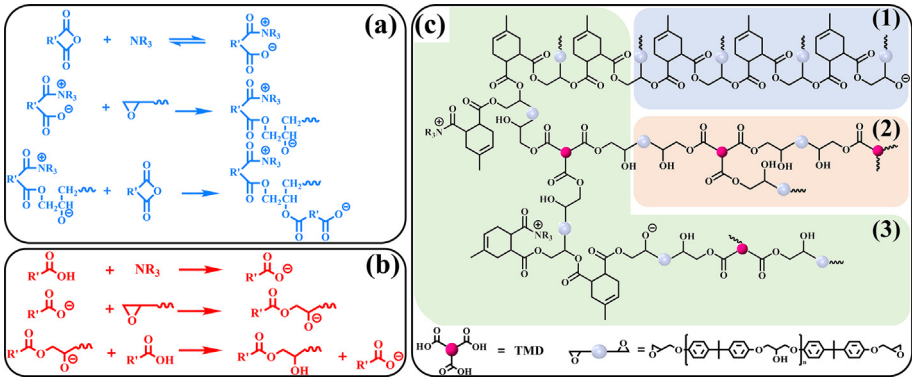

Scheme 2. Reaction mechanisms of epoxy with anhydride (a) and carboxylic acid (b) catalyzed by tertiary amine; and the corresponding crosslinking system of this study (c).

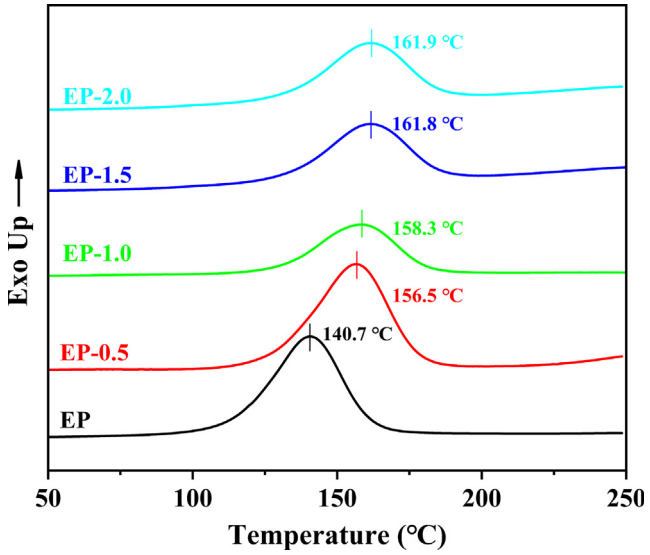

Fig. 3. DSC heating scans of EP and FREP.

This was attributed to the stable chemical combination of flame retardant and epoxy chain after the cross-linking reaction. In addition, the R_{max} decreased from 14.5%/min of pure EP to 12.3%/min of EP-2.0, which further revealed that FREP maintained good thermal stability. Furthermore, the char residue at 800 °C significantly increased from 6.5% for pure EP to 16.7% for EP-2.0, with a 157% relative increment, which meant that TMD exhibited excellent char-forming ability. In contrast, EP-DOPO sample left only 5.9% char residue which was lower than that of pure EP. This result was mainly attributed to the fact that on one hand, DOPO exerted more effect in gas phase and relatively less effect on carbonization. On the other hand, $T_{5\%}$ of EP-DOPO sample declined by 67.7 °C compared with pure EP, indicating that the excessive incorporation of DOPO weakened the thermal stability of EP seriously. This suggested that DOPO promoted EP matrix to decompose in advance to produce more volatiles, which also made a negative effect on the increase of char residue. All these results indicated that compared with DOPO, TMD had little effect on thermal stability of EP and behaved more efficient char-forming ability.

In order to further prove the char-forming ability of TMD, the experimental and calculated curves (assuming that EP and TMD decomposed respectively) as well as the detailed data were exhibited in Fig. 5c, d and Table 3, respectively. In terms of TMD, it experienced three degradation stages with T_{max} at 204.5/415.7/441.7 °C, finally leaving 14.9% char residue. The earliest mass loss corresponded to dehydration or decarboxylation of carboxylic acid group. The rest two stages were the main degradation processes of TMD, where the second stage was ascribed to the decomposition of less stable DOPO group and immediately followed by the degradation of triazine-trione group [23]. The decomposition route of TMD will be further investigated in the following study. Compared to calculated curves, $T_{5\%}$ of Exp-EP/TMD was higher owing to the reaction of carboxyl and epoxy group. Additionally, T_{max} of Exp-EP/TMD was lower than the corresponding calculated value, while the char residue of Exp-EP/TMD was dramatically elevated from 8.7% of Cal-EP/TMD to 16.7%. Those results suggested that the introduction of TMD promoted the degradation of EP matrix at a relative lower temperature. The pyrolytic products of TMD can accelerate carbonization of EP matrix to form more char residues to inhibit degradation. Therefore, FREP possessed high thermal stability at a high temperature and can yield more char residue finally.

3.4. Flame retardance and combustion behavior

The flame retardance of FREP was measured by LOI and UL-94 tests, and the corresponding results were exhibited in Table 4. It was seen that the LOI value of pure EP was just 20.1%, which was much lower than that of amine-cured EP of 22.5% [42], indicating that anhydride-cured EP is particularly easy to combust. Nevertheless, when introducing the flame retardant, higher LOI values were obtained, implying the improvement of flame retardancy of EP. The LOI value of EP-0.5 sample loaded with only 0.5 wt% phosphorus increased to 25.0%, but the sample failed to pass the UL-94 burning test. As the phosphorus content increased, the LOI value was gradually improved. When the phosphorus

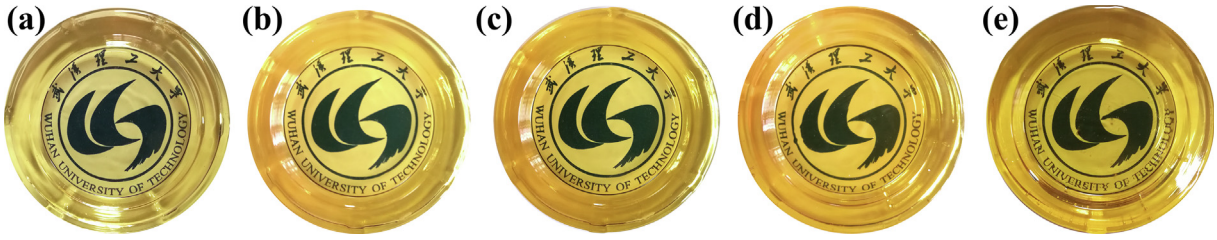

Fig. 4. Digital photos of EP (a), EP-0.5 (b), EP-1.0 (c), EP-1.5 (d) and EP-2.0 (e).

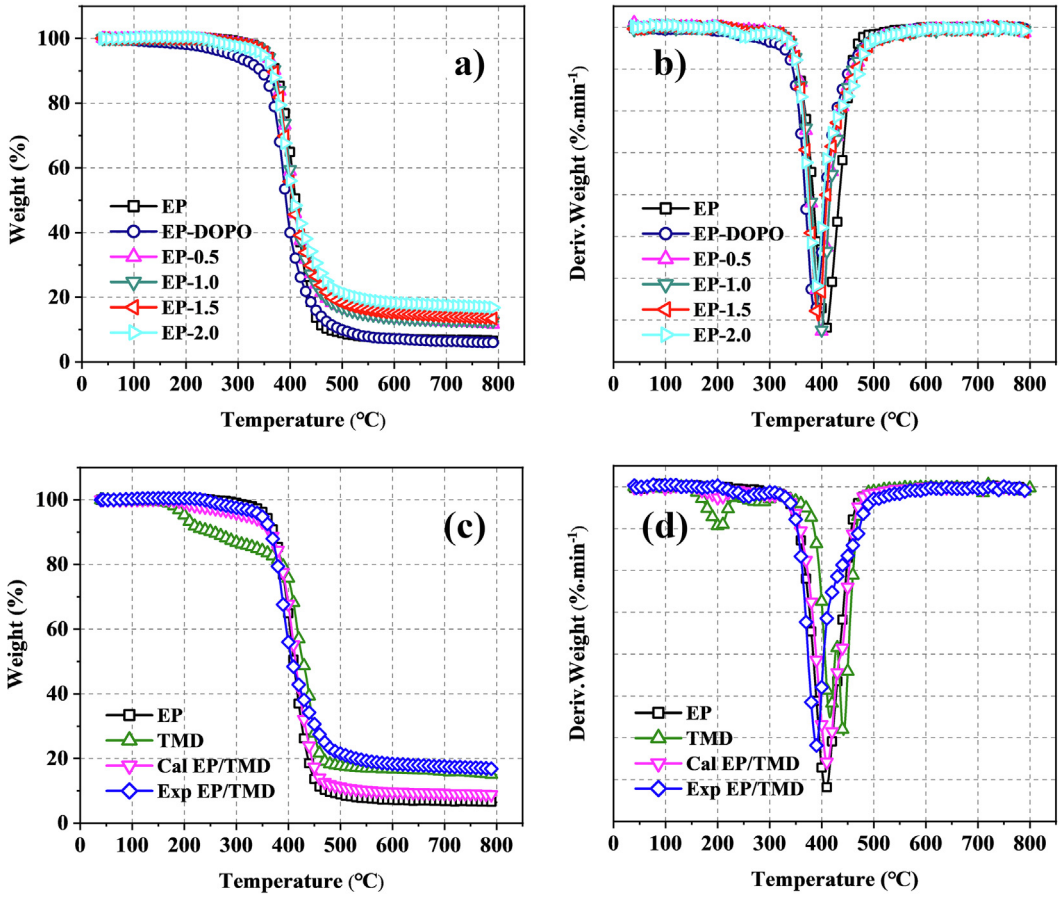

Fig. 5. TG (a, c) and DTG (b, d) curves of the EP, FREP, Cal-EP/TMD and Exp-EP/TMD.

Table 2
Thermogravimetric data of EP and FREP.

Sample	$T_{5\%}$ (°C)	T_{max} (°C)	R_{max} (%/min)	Char residue at 800 °C (%)
EP	356.9	407.5	14.5	6.5
EP-DOPO	289.2	387.2	13.6	5.9
EP-0.5	356.3	398.2	14.6	11.5
EP-1.0	354.9	398.0	14.6	12.5
EP-1.5	354.0	393.2	13.9	13.3
EP-2.0	348.7	389.7	12.3	16.7

Table 3
Thermogravimetric data of EP, TMD, Cal-EP/TMD and Exp-EP/TMD.

Sample	$T_{5\%}$ (°C)	T_{max} (°C)	Char residue at 800 °C (%)
EP	356.9	407.5	6.5
TMD	201.3	204.5/415.7/441.7	14.9
Cal-EP/TMD	316.4	409.6	8.7
Exp-EP/TMD	348.7	389.7	16.7

Table 4
Flammability test results of EP and FREP.

Sample	LOI (%)	UL-94 (3 mm)	Dripping
EP	20.1	NR[a]	Yes
EP-DOPO	31.9	V-1	No
EP-0.5	25.0	NR	No
EP-1.0	28.3	V-1	No
EP-1.5	30.7	V-1	No
EP-2.0	32.8	V-0	No

[a] No rating.

content was raised to 1.0 wt%, the LOI value of EP-1.0 sample was as high as 28.3%, and it passed UL-94 V-1 rating. If further increasing the phosphorus content, EP-2.0 sample (2.0 wt% phosphorous loading) can acquire the maximum LOI value of 32.8%, with a 63.2% increment compared to pure EP, and can achieve V-0 rating easily. However, EP-DOPO sample (the same phosphorus content as EP-2.0 sample) can only pass UL-94 V-1 rating, although its LOI value was 31.9%. This indicated that simultaneous introduction of phosphaphenanthrene and triazine-trione groups can further improve flame retardancy of EP. Thus, it can be concluded that TMD was a more efficient flame retardant than DOPO for anhydride-cured EP.

The cone calorimeter (CC), imitating the real fire conditions, has been widely used to evaluate the flammability as well as potential fire safety of polymeric materials, and provides a series of parameters on flammability characteristics of materials [43,44]. The heat release rate (HRR), total heat release (THR) and mass curves as a function of time and corresponding data were shown in Fig. 6 and Table 5, respectively.

Time to ignition (TTI) is the critical indicator to evaluate the impact of flame retardants on flammability of cured EP. As revealed in Table 5, TTI of the FREP increased compared to pure EP. Based on the analysis of TGA, this phenomenon may be attributed to the fact that the early degradation of TMD produces some volatile substances, which can dilute the concentration of oxygen and take away the heat [22,45]. Therefore, the FREP possessed higher ignition-resistance.

The HRR can evaluate how fast flame grows during combustion and quantify the size of the fire. It can be seen from Fig. 6a that pure EP burned fiercely after ignition and reached the peak heat release rate (PHRR) of 1149.8 kW/m^2. While after the incorporation of TMD, the PHRR of EP-2.0 was sharply decreased to 467.7 kW/m^2, corresponding to a 59.3% reduction. Similar to the HRR, the THR of FREP significantly reduced from 86.3 MJ/m^2 of pure EP to 59.1 MJ/m^2 of EP-2.0,

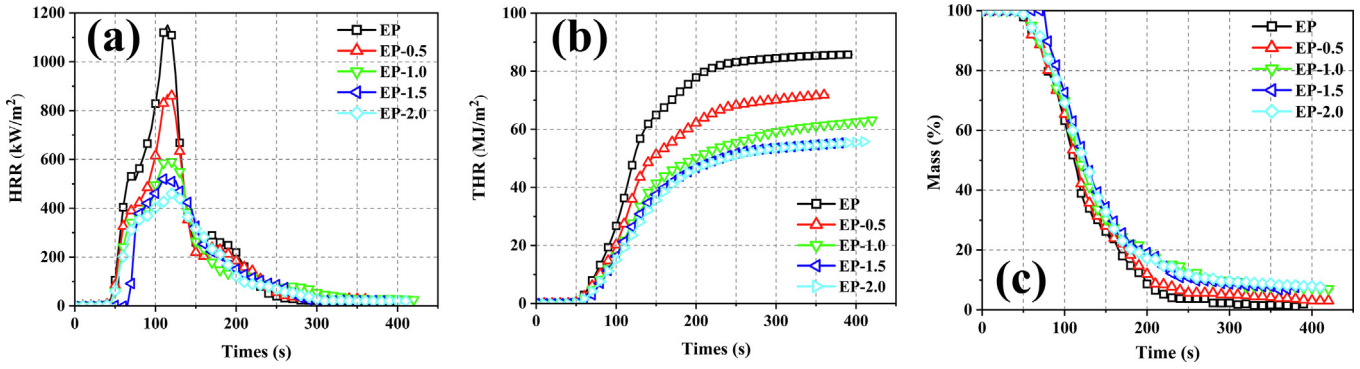

Fig. 6. HRR (a), THR (b) and mass (c) curves of EP and FREP obtained from cone calorimetry.

indicating that TMD can effectively enhance the flame retardancy of EP. In general, the fire growth rate (FIGRA), the ratio of PHRR to TTPHRR (time to PHRR), can be used to evaluate the fire hazard of the materials [46]. It was observed that FIGRA of EP-2.0 dropped to 3.7 kW/m^2·s, which was much lower than that of pure EP of 10.0 kW/m^2·s. Lower FGIRA means the longer time to arrive at PHRR, thus there are more time for people to evacuate from a fire accident.

In addition, the effective heat of combustion (EHC), defined as the ratio of heat release to mass loss at a certain time during combustion, can exactly reveal the burning degree of volatiles in gas phase. As shown in Table 5, averaged EHC (av-EHC) decreased from 20.9 MJ/kg for pure EP to 14.5 MJ/kg for EP-2.0, which was attributed to the increase of concentration of noncombustible gas and the incomplete combustion of volatiles in gas phase [45,47]. In detail, on one hand, the cured EP containing DOPO group and nitrogenous heterocyclic structure can release noncombustible gases such as volatile phosphide, N_2, NH_3 and NO_2 during the combustion. On the other hand, the decomposition of DOPO group can release phosphorus-containing free radicals to interrupt free radical chain reaction [46,48], finally causing the incomplete combustion of volatiles in gas phase. It was also reflected in the increase of average CO yield (av-COY) and the reduction of average CO_2 yield (av-CO_2Y), as presented in Table 5, since CO and CO_2 correspond to the incomplete and complete combustion products, respectively. Moreover, total smoke production (TSP) of FREP increased because of the incomplete combustion of polycyclic aromatic hydrocarbon cracked from the matrix, which indicated that the flame-retardant mechanism of TMD can be mainly ascribed to gas phase flame inhibition [49–51]. Furthermore, char residue increased from 2.0% of pure EP to 7.7% of EP-2.0, indicating the incorporation of TMD promoted the formation of char residue, which is consistent with the results of TGA. To our best knowledge, the stable char layer can act as a good heat isolating layer to hinder the transfer of heat and oxygen into the underlying matrix during combustion, which is of great help to inhibit the further burning of EP. Consequently, based on the above analysis of results, it is reasonable to believe that TMD can exhibit main flame-retardant effects in gas phase and can also play a role in the condensed phase.

3.5. Analysis on char residue

The digital photos and SEM images of char residues after cone calorimeter tests for pure EP, EP-1.0 and EP-2.0 were exhibited in Fig. 7. As presented in Fig. 7a_1, pure EP burned completely and left nearly no char residue after the cone calorimetry test, whereas the FREP yielded more char residue shown in Fig. 7b_1, c_1. As for the SEM images, the discontinuous structure and numerous tiny holes on the char surface of pure EP can be clearly observed. The hole on the char residue is beneficial for the release of combustible volatiles from the internal matrix to the gas phase. As a result, pure EP behaved higher HRR and THR values. However, the char surface became compact and continuous after the incorporation of TMD. More interestingly, compared to EP-1.0, it was found that there were many intact and intumescent bubbles on the continuous char surface of EP-2.0, rather than the broken bubble structures destroyed by gas flow and heat flux, which suggested with the increase of content of TMD, the thermal stability of char layer was enhanced. Such compact and thermal-stable char layer can greatly act as a protective barrier to prevent the underlying materials from further decomposing and limit the transfer of combustible volatiles as well as heat between gas and condensed phases.

Raman spectroscopy was used to investigate the structure of carbonaceous materials. The spectrum usually exhibits two remarkable overlapping peaks at 1360 cm^{-1} (D band) and 1590 cm^{-1} (G band), which correspond to the disordered graphite or glassy carbons and organized graphitic structure, respectively. Normally, the integral intensity ratio of the two bands (I_D/I_G) can reflect the graphitization degree of char residue. A lower I_D/I_G value represents a higher graphitization degree [52]. As shown in Fig. 8, the I_D/I_G value for EP-2.0 was much lower than that of pure EP, demonstrating the improved graphitization degree of char residue. It means that after the addition of TMD, the cured EP can form a more stable char layer, which coincides with the result observed in the SEM.

To further reveal the flame-retardant mechanism of TMD in condensed phase, the FTIR spectra of the char residue was analyzed and presented in Fig. 9. Through the analysis of reactions of epoxy with anhydride, it can be found that there are numerous ester bonds in the anhydride-cured EP. However, no characteristic absorption peak of carbonyl was found in the FTIR spectra of char residue of pure EP, indicating that the ester bonds decomposed almost completely.

Table 5
Cone calorimetric test results of EP and FREP.

Sample	TTI (s)	PHRR (kW/m^2)	THR (MJ/m^2)	TTPHRR (s)	FIGRA (kW/m^2·s)	av-EHC (MJ/kg)	av-COY (kg/kg)	av-CO_2Y (kg/kg)	TSP (m^2)	Char residue (%)
EP	28	1149.8	86.3	115	10.0	20.9	0.065	1.959	32.2	2.0
EP-0.5	28	865.1	76.5	115	7.5	18.3	0.108	1.582	37.0	3.1
EP-1.0	30	603.4	67.6	115	5.2	16.8	0.120	1.477	40.0	6.8
EP-1.5	64	519.5	59.2	110	4.7	14.5	0.137	1.322	41.2	7.6
EP-2.0	40	467.7	59.1	125	3.7	14.5	0.160	1.317	41.7	7.7

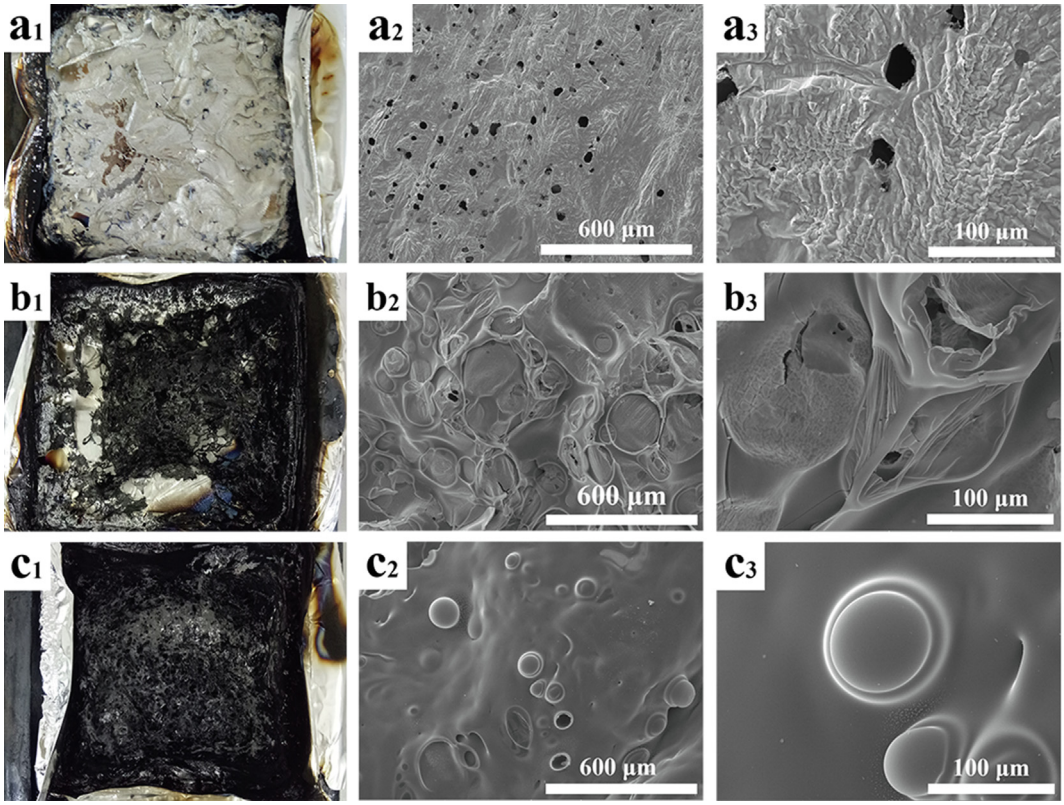

Fig. 7. Digital photos and SEM images of the char residues of EP (a), EP-1.0 (b) and EP-2.0 (c) after cone calorimeter tests; Subscript 1 represents the digital photo, 2 indicates the SEM images (×200) and 3 stands for the local magnified SEM images (×1000).

Nevertheless, after the addition of TMD, the peaks corresponding to C=O and C-N appeared at around 1700 and 1376 cm^{-1}, respectively. This demonstrated that triazine-trione structure existed in char residue of EP-2.0 sample, suggesting the high thermal stability of triazine-trione group from the side. Meantime, new absorption peak at 1200 cm^{-1} which can be attributed to P=O appeared. These results suggested that those phosphorus and nitrogen-containing compounds from the thermal decomposition of TMD can promote EP matrix to form a more compact and stable char layer.

3.6. Pyrolysis behavior

To further investigate pyrolysis behavior and the flame-retardant mechanism in gas phase, Py-GC/MS was adopted to analyze the volatile products. The total ion chromatograms of TMD was shown in Fig. 10a. According to the structure of TMD, MS spectrum at 23.9 min shown in Fig. 10b, which contained typical fragment flow with plenty of characteristic ionic peaks, was selected to analyze the pyrolysis route of TMD. The presumptive pyrolytic route was presented in Scheme 3. The decomposition products of TMD can be mainly classified as phosphaphenanthrene fragment, tri-ethylethyl-triazine-trione fragment and carboxylic acid fragment. Thereafter, those three fragments further separately decomposed to generate smaller molecular weight compounds. The phosphaphenanthrene fragment pyrolyzed into o-phenylphenol (m/z = 170), o-phenylphenoxyl free radical (m/z = 169), dibenzofuran (m/z = 168), biphenyl free radical (m/z = 152), O=P−O−Ph free radical (m/z = 139, 141) and PO_2 free radical (m/z = 63). In addition, the tri-ethylethyl-triazine-trione fragment degraded into nitrogen-containing compounds (m/z = 69, 43) and active allyl radical (m/z = 41) which finally transformed to cyclopropylium

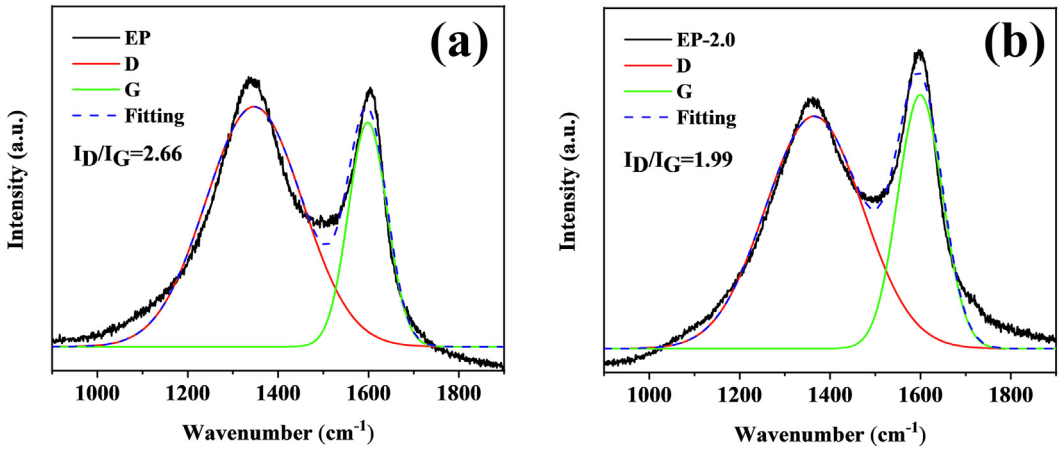

Fig. 8. Raman spectra of char residues for EP (a) and EP-2.0 (b).

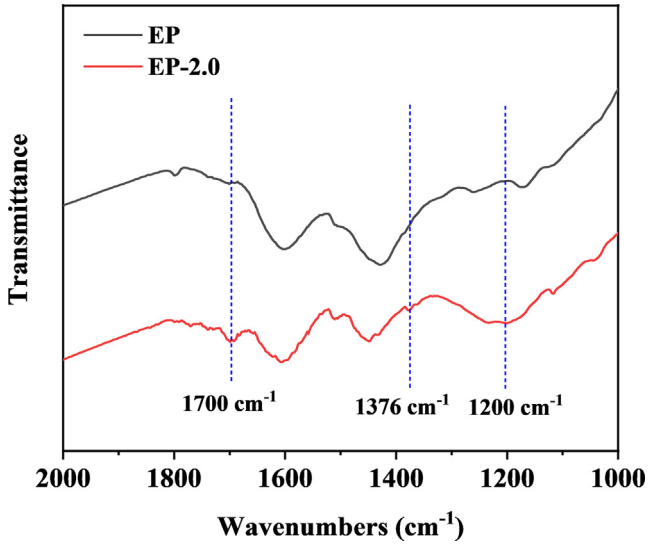

Fig. 9. FTIR spectra of char residues for EP and EP-2.0.

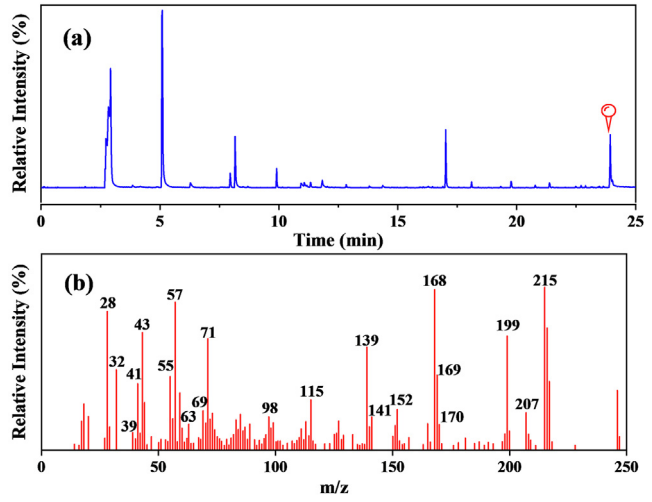

Fig. 10. Total ion chromatogram (a) and typical MS spectrum of main fragments of the pyrolyzed TMD at 500 °C (b).

(m/z = 39). Since the TMD participated in the curing of EP, only the decomposition of carboxylic acid fragment changed. Thus, TMD cured into epoxy networks could also produce those phosphorus-containing and nitrogen-containing compounds. On one hand, phosphorus-containing compounds such as $\cdot PO_2$ free radical can capture and quench ·H and ·OH free radicals, thereby interrupting free radical chain reaction and suppressing the burning intensity during combustion. On the other hand, nitrogen-containing nonflammable compounds produced by the decomposition of triazine-trione fragment can make contributions to dilute the concentration of oxygen around the flame as well as the combustible gases released by the matrix, and take away the burning heat.

3.7. Flame-retardant mechanism

Based on the analysis mentioned above, it can be concluded that TMD exerts flame-retardant mechanism both in gas phase and condensed phase, and the flame-retardant mechanism was summarized as Fig. 11. In gas phase, flame-retardant mechanism origins from the quenching effect of phosphorus-containing free radicals and dilution action of nonflammable gas mainly released by the nitrogen-containing compounds which will also take away the burning heat. In condensed phase, the formed phosphoric acids catalyze the dehydration and carbonization of the matrix to form compact and stable char layer which obstructs the transfer of combustible volatiles and heat. Simultaneously, the heat-resistant triazine-trione group participates in carbonization to protect the matrix from further decomposition. Therefore, the synergistic effect between phosphaphenanthrene and triazine-trione groups endows FREP with excellent flame retardance.

3.8. Dynamic mechanical analysis and mechanical properties

Dynamic mechanical behavior of cured EP was investigated by DMA. The storage modulus and tan delta curves as a function of temperature for EP and FREP were illustrated in Fig. 12, and the corresponding data were listed in Table 6. As the content of TMD increased, the storage modulus at 50 °C showed an increasing trend from 2431 MPa of pure EP to 2701 MPa of EP-2.0, indicating that TMD served as a fortifier for improving the modulus of EP. However, the T_g values (the peak temperature of tan delta) of the cured EP slightly decreased with the increasing content of TMD. Generally, the introduction of the rigid group should restrain the mobility of macromolecular chains and lead to the increase of T_g. To better explain this phenomenon, the crosslinking density (ν_e) was introduced. According to the

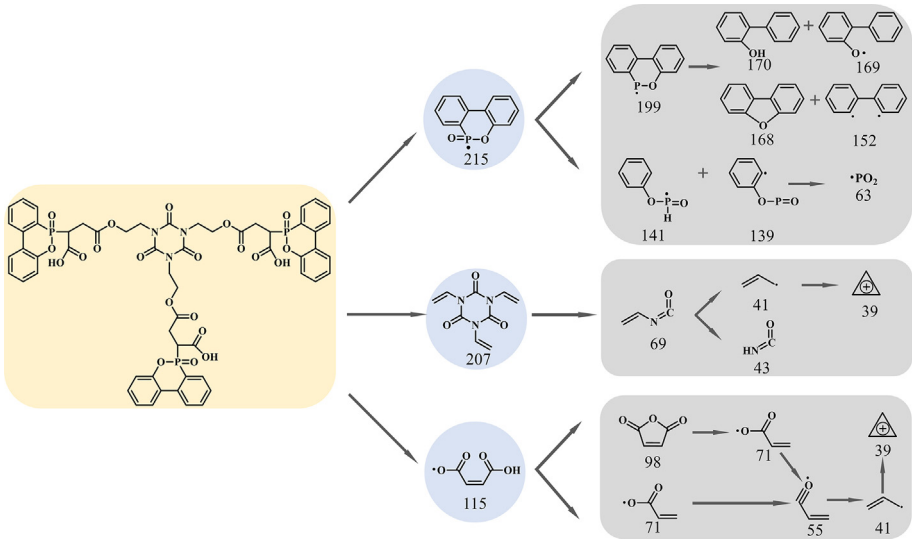

Scheme 3. Proposed pyrolitic route of TMD.

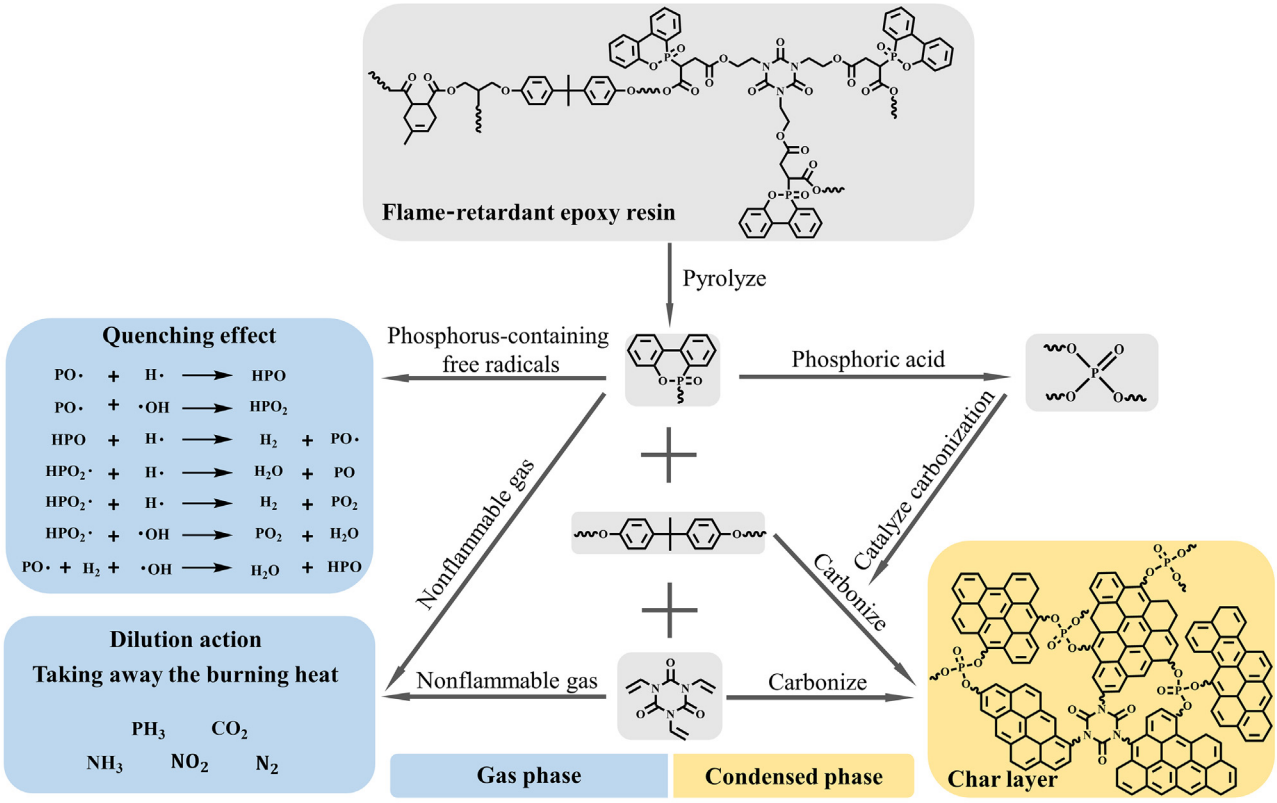

Fig. 11. Schematic illustration of the flame-retardant mechanism of FREP.

literature [53], ν_e can be calculated by the rubber elasticity theory with the Eq. (1).

$$\nu_e = E'/3RT \quad (1)$$

where E' is the storage modulus at T_g + 40 °C in the rubbery plateau, R is the ideal gas constant (8.314 J/K·mol) and T is the thermodynamic temperature at T_g + 40 °C. As shown in Table 6, crosslinking density of cured EP decreased as the content of TMD increased. This was because that in addition to rigid DOPO and triazine-trione groups, the polyfunctionality and long flexible aliphatic chain also existed in the structure of TMD, which allowed the crosslinking network of epoxy to exhibit a hyperbranched structure, thus resulting in the decrease of crosslink density [54]. From the above results, it can be inferred that the reduction of crosslinking density was the leading cause of the decrease of T_g.

Furthermore, the mechanical properties of EP and FREP were evaluated by flexural and tensile tests. The typical strain-stress curves of the cured EP and detailed data were presented in Fig. 13. It can be observed that most of the FREP showed higher flexural and tensile modulus than pure EP due to the introduction of rigid groups. Likewise, except the EP-2.0 sample, their flexural and tensile strength also improved slightly compared with pure EP. Normally, without changing

Table 6
Thermomechanical properties of EP and FREP.

Sample	T_g (°C)	Storage modulus at 50 °C (MPa)	$\nu_e \times 10^{-3}$(mol/m^3)
EP	138	2431	2.78
EP-0.5	135	2622	2.38
EP-1.0	133	2607	1.96
EP-1.5	131	2681	1.94
EP-2.0	130	2701	1.45

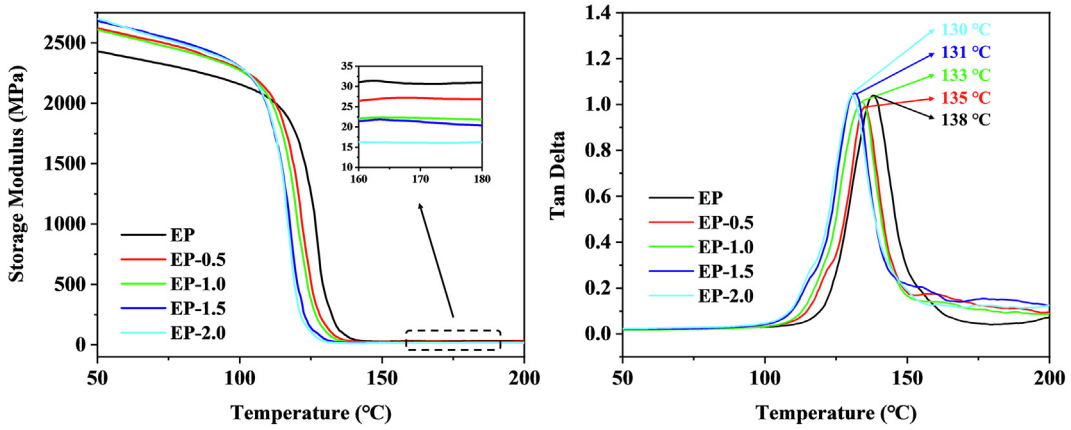

Fig. 12. DMA curves of EP and FREP.

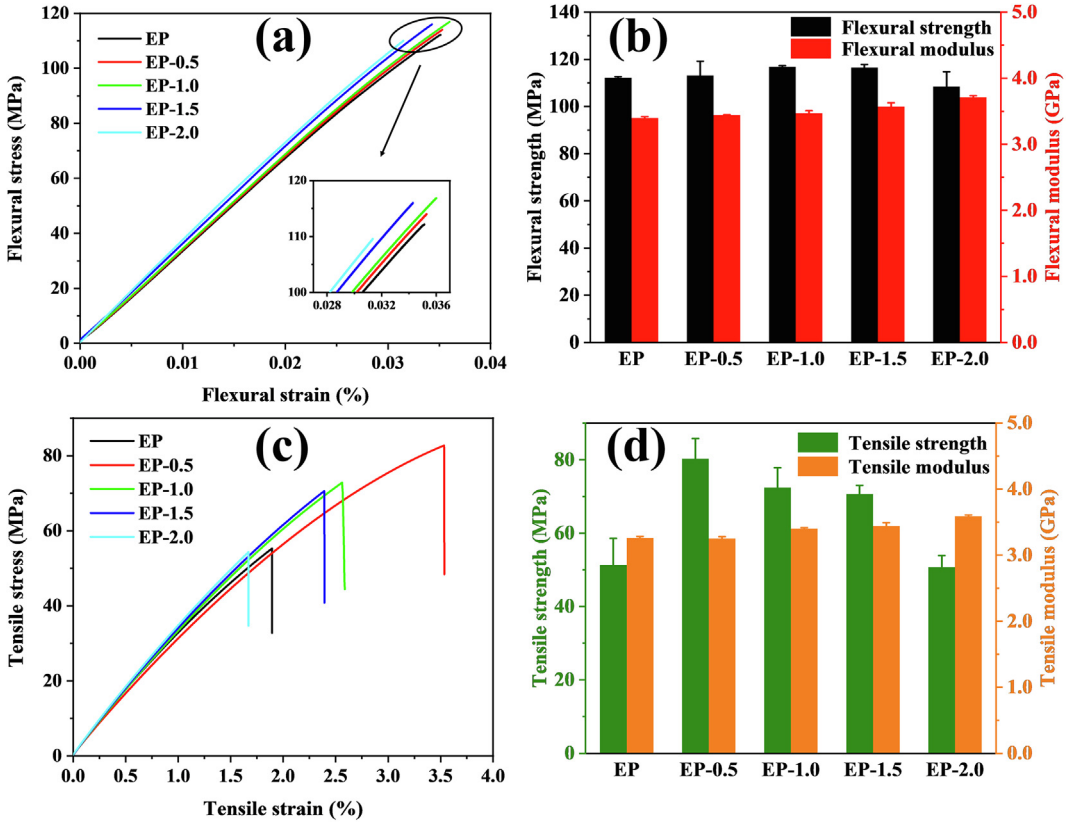

Fig. 13. Stress-strain curves (a, c) and strength as well as modulus (b, d) of EP and FREP.

the crosslinking network, the strength of cured EP is determined by crosslinking density. Nevertheless, three crosslinking networks exist simultaneously after the addition of TMD. On one hand, this heterogeneous network may have a positive impact on mechanical properties of cured EP. On the other hand, more and more hydrogen bonds formed due to the increase of hydroxyl group, which act as the physical crosslinking point to improve mechanical properties [40]. However, the increase of hydrogen bond was unable to compensate for the deterioration of mechanical properties caused by the excessive decrease in crosslinking density. Therefore, the strength of cured EP increased first and then decreased. In summary, the mechanical properties of FREP are enhanced slightly after the incorporation of TMD.

4. Conclusion

In this work, a novel reactive flame retardant TMD simultaneously containing phosphorus and nitrogen has been designed and synthesized successfully via a facile monoesterification and addition reaction between THEIC, MAH and DOPO. It was confirmed by DSC that TMD can participate in the curing reaction of EP together with anhydride curing agent. The obtained FREP presented good transparency owing to the excellent compatibility of TMD with EP. Besides, when the phosphorus content was 2.0 wt%, the LOI value of FREP dramatically improved from 20.1% of pure EP to 32.8%, and UL-94 V-0 rating was achieved. The results of TGA and cone calorimeter demonstrated that FREP maintained good thermal stability with only a little decrease in $T_{5\%}$ and presented higher ignition-resistance as well as much lower PHRR, THR, FIGRA and av-EHC compared with pure EP. Through the studies on char residual of the cured EP and pyrolysis process of TMD, it can be further concluded that TMD exerted flame-retardant mechanism both in gas phase and condensed phase. Moreover, in spite of a lower crosslink density with a slightly decreased T_g, FREP also possessed good mechanical properties due to the formation of heterogeneous network and hydrogen bonding. As a consequence, all the results indicated that this novel flame retardant exhibited great potential applications in the future.

Acknowledgments

This work was supported by the National Natural Science Foundation of China (Grant No. 51573144 and 51303143) and the Fundamental Research Funds for the Central Universities (Grant No. 195201008).

References

[1] X. Zhang, Q. He, H. Gu, H.A. Colorado, S. Wei, Z. Guo, Flame-retardant electrical conductive nanopolymers based on bisphenol F epoxy resin reinforced with nano polyanilines, ACS Appl. Mater. Interfaces 5 (2013) 898–910.
[2] M. Xing, F.-S. Zhang, Degradation of brominated epoxy resin and metal recovery from waste printed circuit boards through batch sub/supercritical water treatments, Chem. Eng. J. 219 (2013) 131–136.
[3] Z. Wang, P. Wei, Y. Qian, J. Liu, The synthesis of a novel graphene-based inorganic–organic hybrid flame retardant and its application in epoxy resin, Compos. Part B 60 (2014) 341–349.
[4] X. Guo, H. Wang, D. Ma, J. He, Z. Lei, Synthesis of a novel, multifunctional inorganic curing agent and its effect on the flame-retardant and mechanical properties of intrinsically flame retardant epoxy resin, J. Appl. Polym. Sci. 135 (2018) 46410.
[5] J. Wan, B. Gan, C. Li, J. Molina-Aldareguia, E.N. Kalali, X. Wang, D.-Y. Wang, A sustainable, eugenol-derived epoxy resin with high biobased content, modulus, hardness and low flammability: synthesis, curing kinetics and structure–property relationship, Chem. Eng. J. 284 (2016) 1080–1093.
[6] S. Qiu, W. Xing, X. Feng, B. Yu, X. Mu, R.K.K. Yuen, Y. Hu, Self-standing cuprous oxide nanoparticles on silica@ polyphosphazene nanospheres: 3D nanostructure for enhancing the flame retardancy and toxic effluents elimination of epoxy resins via synergistic catalytic effect, Chem. Eng. J. 309 (2017) 802–814.
[7] Y. Tan, Z.-B. Shao, L.-X. Yu, J.-W. Long, M. Qi, L. Chen, Y.-Z. Wang, Piperazine-modified ammonium polyphosphate as monocomponent flame-retardant hardener for epoxy resin: flame retardance, curing behavior and mechanical property, Polym. Chem. 7 (2016) 3003–3012.
[8] S. Huo, J. Wang, S. Yang, B. Zhang, X. Chen, Q. Wu, L. Yang, Synthesis of a novel reactive flame retardant containing phosphaphenanthrene and piperidine groups

and its application in epoxy resin, Polym. Degrad. Stab. 146 (2017) 250–259.
[9] A. Covaci, S. Harrad, M.A. Abdallah, N. Ali, R.J. Law, D. Herzke, C.A. de Wit, Novel brominated flame retardants: a review of their analysis, environmental fate and behaviour, Environ. Int. 37 (2011) 532–556.
[10] S. Ling, K. Huang, M. Tariq, Y. Wang, X. Chen, W. Zhang, K. Lin, B. Zhou, Photodegradation of novel brominated flame retardants (NBFRs) in a liquid system: kinetics and photoproducts, Chem. Eng. J. 362 (2019) 938–946.
[11] Y. Shi, G. Wang, The novel epoxy/PEPA phosphate flame retardants: synthesis, characterization and application in transparent intumescent fire resistant coatings, Prog. Org. Coat. 97 (2016) 1–9.
[12] K.N. Bauer, H.T. Tee, M.M. Velencoso, F.R. Wurm, Main-chain poly(phosphoester)s: History, syntheses, degradation, bio-and flame-retardant applications, Prog. Polym. Sci. 73 (2017) 61–122.
[13] Y. Tan, Z.-B. Shao, L.-X. Yu, Y.-J. Xu, W.-H. Rao, L. Chen, Y.-Z. Wang, Polyethyleneimine modified ammonium polyphosphate toward polyamine-hardener for epoxy resin: thermal stability, flame retardance and smoke suppression, Polym. Degrad. Stab. 131 (2016) 62–70.
[14] X. Mu, J. Zhan, X. Feng, B. Yuan, S. Qiu, L. Song, Y. Hu, Novel Melamine/o-Phthalaldehyde Covalent Organic Frameworks Nanosheets: Enhancement Flame Retardant and Mechanical Performances of Thermoplastic Polyurethanes, ACS Appl. Mater. Interfaces 9 (2017) 23017–23026.
[15] S. Yang, Q. Zhang, Y. Hu, Synthesis of a novel flame retardant containing phosphorus, nitrogen and boron and its application in flame-retardant epoxy resin, Polym. Degrad. Stab. 133 (2016) 358–366.
[16] S. Qiu, Y. Hou, W. Xing, C. Ma, X. Zhou, L. Liu, Y. Kan, R.K.K. Yuen, Y. Hu, Self-assembled supermolecular aggregate supported on boron nitride nanoplatelets for flame retardant and friction application, Chem. Eng. J. 349 (2018) 223–234.
[17] C. Liu, T. Chen, C.H. Yuan, C.F. Song, Y. Chang, G.R. Chen, Y.T. Xu, L.Z. Dai, Modification of epoxy resin through the self-assembly of a surfactant-like multi-element flame retardant, J. Mater. Chem. A 4 (2016) 3462–3470.
[18] X. Qian, L. Song, Y. Bihe, B. Yu, Y. Shi, Y. Hu, R.K.K. Yuen, Organic/inorganic flame retardants containing phosphorus, nitrogen and silicon: preparation and their performance on the flame retardancy of epoxy resins as a novel intumescent flame retardant system, Mater. Chem. Phys. 143 (2014) 1243–1252.
[19] Y. Tan, Z.B. Shao, X.F. Chen, J.W. Long, L. Chen, Y.Z. Wang, Novel Multifunctional Organic-Inorganic Hybrid Curing Agent with High Flame-Retardant Efficiency for Epoxy Resin, ACS Appl. Mater. Interfaces 7 (2015) 17919–17928.
[20] Y. Feng, C. He, Y. Wen, Y. Ye, X. Zhou, X. Xie, Y.-W. Mai, Improving thermal and flame retardant properties of epoxy resin by functionalized graphene containing phosphorous, nitrogen and silicon elements, Compos. Part A 103 (2017) 74–83.
[21] X.-Y. Jian, Y. He, Y.-D. Li, M. Wang, J.-B. Zeng, Curing of epoxidized soybean oil with crystalline oligomeric poly(butylene succinate) towards high performance and sustainable epoxy resins, Chem. Eng. J. 326 (2017) 875–885.
[22] Y.-Q. Shi, T. Fu, Y.-J. Xu, D.-F. Li, X.-L. Wang, Y.-Z. Wang, Novel phosphorus-containing halogen-free ionic liquid toward fire safety epoxy resin with well-balanced comprehensive performance, Chem. Eng. J. 354 (2018) 208–219.
[23] S. Yang, J. Wang, S. Huo, M. Wang, L. Cheng, Synthesis of a Phosphorus/Nitrogen-Containing Additive with Multifunctional Groups and Its Flame-Retardant Effect in Epoxy Resin, Ind. Eng. Chem. Res. 54 (2015) 7777–7786.
[24] K.A. Salmeia, S. Gaan, An overview of some recent advances in DOPO-derivatives: chemistry and flame retardant applications, Polym. Degrad. Stab. 113 (2015) 119–134.
[25] R. Jian, P. Wang, L. Xia, X. Zheng, Effect of a novel P/N/S-containing reactive flame retardant on curing behavior, thermal and flame-retardant properties of epoxy resin, J. Anal. Appl. Pyrolysis 127 (2017) 360–368.
[26] I.-D. Carja, D. Serbezeanu, T. Vlad-Bubulac, C. Hamciuc, A. Coroaba, G. Lisa, C.G. López, M.F. Soriano, V.F. Pérez, M.D. Romero, Sánchez, A straightforward, eco-friendly and cost-effective approach towards flame retardant epoxy resins, J. Mater. Chem. A 2 (2014) 16230–16241.
[27] T. Ma, C. Guo, Synergistic effect between melamine cyanurate and a novel flame retardant curing agent containing a caged bicyclic phosphate on flame retardancy and thermal behavior of epoxy resins, J. Anal. Appl. Pyrolysis 124 (2017) 239–246.
[28] S. Khanal, W. Zhang, S. Ahmed, M. Ali, S. Xu, Effects of intumescent flame retardant system consisting of tris (2-hydroxyethyl) isocyanurate and ammonium polyphosphate on the flame retardant properties of high-density polyethylene composites, Compos. Part A 112 (2018) 444–451.
[29] L. Qian, Y. Qiu, N. Sun, M. Xu, G. Xu, F. Xin, Y. Chen, Pyrolysis route of a novel flame retardant constructed by phosphaphenanthrene and triazine-trione groups and its flame-retardant effect on epoxy resin, Polym. Degrad. Stab. 107 (2014) 98–105.
[30] S. Huo, J. Wang, S. Yang, J. Wang, B. Zhang, B. Zhang, X. Chen, Y. Tang, Synthesis of a novel phosphorus-nitrogen type flame retardant composed of maleimide, triazine-trione, and phosphaphenanthrene and its flame retardant effect on epoxy resin, Polym. Degrad. Stab. 131 (2016) 106–113.
[31] X. Tao, H. Duan, W. Dong, X. Wang, S. Yang, Synthesis of an acrylate constructed by phosphaphenanthrene and triazine-trione and its application in intrinsic flame retardant vinyl ester resin, Polym. Degrad. Stab. 154 (2018) 285–294.
[32] A. omrani, A.A. Rostami, F. Ravari, A. Mashak,, Curing behavior and structure of a novel nanocomposite from glycerol diglycidyl ether and 3,3-dimethylglutaric anhydride, Thermochim. Acta 517 (2011) 9–15.
[33] T. Yang, C. Zhang, J. Zhang, J. Cheng, The influence of tertiary amine accelerators on the curing behaviors of epoxy/anhydride systems, Thermochim. Acta 577 (2014) 11–16.
[34] H. Gu, J. Guo, H. Wei, X. Yan, D. Ding, X. Zhang, Q. He, S. Tadakamalla, X. Wang, T.C. Ho, S. Wei, Z. Guo, Transparent anhydride–cured epoxy nanocomposites reinforced with polyaniline stabilized nanosilica, J. Mater. Chem. C 3 (2015) 8152–8165.
[35] M. Fan, J. Liu, X. Li, J. Zhang, J. Cheng, Thermal, mechanical and shape memory properties of an intrinsically toughened epoxy/anhydride system, J. Polym. Res. 21 (2014).
[36] M.P. Luda, A.I. Balabanovich, M. Zanetti, Pyrolysis of fire retardant anhydride-cured epoxy resins, J. Anal. Appl. Pyrolysis 88 (2010) 39–52.
[37] Y.-J. Xu, L. Chen, W.-H. Rao, M. Qi, D.-M. Guo, W. Liao, Y.-Z. Wang, Latent curing epoxy system with excellent thermal stability, flame retardance and dielectric property, Chem. Eng. J. 347 (2018) 223–232.
[38] D. Foix, Y. Yu, A. Serra, X. Ramis, J.M. Salla, Study on the chemical modification of epoxy/anhydride thermosets using a hydroxyl terminated hyperbranched polymer, Eur. Polym. J. 45 (2009) 1454–1466.
[39] D. Foix, M.T. Rodríguez, F. Ferrando, X. Ramis, A. Serra, Combined use of sepiolite and a hyperbranched polyester in the modification of epoxy/anhydride coatings: a study of the curing process and the final properties, Prog. Org. Coat. 75 (2012) 364–372.
[40] Z.-B. Shao, M.-X. Zhang, Y. Li, Y. Han, L. Ren, C. Deng, A novel multi-functional polymeric curing agent: synthesis, characterization, and its epoxy resin with simultaneous excellent flame retardance and transparency, Chem. Eng. J. 345 (2018) 471–482.
[41] X. Qian, L. Song, Y. Hu, R.K.K. Yuen, L. Chen, Y. Guo, N. Hong, S. Jiang, Combustion and Thermal Degradation Mechanism of a Novel Intumescent Flame Retardant for Epoxy Acrylate Containing Phosphorus and Nitrogen, Ind. Eng. Chem. Res. 50 (2011) 1881–1892.
[42] S. Tang, L. Qian, X. Liu, Y. Dong, Gas-phase flame-retardant effects of a bi-group compound based on phosphaphenanthrene and triazine-trione groups in epoxy resin, Polym. Degrad. Stab. 133 (2016) 350–357.
[43] W. Xing, W. Yang, W. Yang, Q. Hu, J. Si, H. Lu, B. Yang, L. Song, Y. Hu, R.K.K. Yuen, Functionalized Carbon Nanotubes with Phosphorus- and Nitrogen-Containing Agents: Effective Reinforcer for Thermal, Mechanical, and Flame-Retardant Properties of Polystyrene Nanocomposites, ACS Appl. Mater. Interfaces 8 (2016) 26266–26274.
[44] Q. Tai, R.K.K. Yuen, L. Song, Y. Hu, A novel polymeric flame retardant and exfoliated clay nanocomposites: preparation and properties, Chem. Eng. J. 183 (2012) 542–549.
[45] R. Jian, P. Wang, W. Duan, J. Wang, X. Zheng, J. Weng, Synthesis of a Novel P/N/S-Containing Flame Retardant and Its Application in Epoxy Resin: Thermal Property, Flame Retardance, and Pyrolysis Behavior, Ind. Eng. Chem. Res. 55 (2016) 11520–11527.
[46] D. Shen, Y.-J. Xu, J.-W. Long, X.-H. Shi, L. Chen, Y.-Z. Wang, Epoxy resin flame-retarded via a novel melamine-organophosphinic acid salt: thermal stability, flame retardance and pyrolysis behavior, J. Anal. Appl. Pyrolysis 128 (2017) 54–63.
[47] M.-J. Xu, G.-R. Xu, Y. Leng, B. Li, Synthesis of a novel flame retardant based on cyclotriphosphazene and DOPO groups and its application in epoxy resins, Polym. Degrad. Stab. 123 (2016) 105–114.
[48] J. Wang, C. Ma, P. Wang, S. Qiu, W. Cai, Y. Hu, Ultra-low phosphorus loading to achieve the superior flame retardancy of epoxy resin, Polym. Degrad. Stab. 149 (2018) 119–128.
[49] N. Wu, G. Fu, Y. Yang, M. Xia, H. Yun, Q. Wang, Fire safety enhancement of a highly efficient flame retardant poly(phenylphosphoryl phenylenediamine) in biodegradable poly(lactic acid), J. Hazard. Mater. 363 (2019) 1–9.
[50] W.-H. Rao, H.-X. Xu, Y.-J. Xu, M. Qi, W. Liao, S. Xu, Y.-Z. Wang, Persistently flame-retardant flexible polyurethane foams by a novel phosphorus-containing polyol, Chem. Eng. J. 343 (2018) 198–206.
[51] Y.-J. Xu, J. Wang, Y. Tan, M. Qi, L. Chen, Y.-Z. Wang, A novel and feasible approach for one-pack flame-retardant epoxy resin with long pot life and fast curing, Chem. Eng. J. 337 (2018) 30–39.
[52] J.-N. Wu, L. Chen, T. Fu, H.-B. Zhao, D.-M. Guo, X.-L. Wang, Y.-Z. Wang, New application for aromatic Schiff base: high efficient flame-retardant and anti-dripping action for polyesters, Chem. Eng. J. 336 (2018) 622–632.
[53] D. Zhao, J. Wang, X.-L. Wang, Y.-Z. Wang, Highly thermostable and durably flame-retardant unsaturated polyester modified by a novel polymeric flame retardant containing Schiff base and spirocyclic structures, Chem. Eng. J. 344 (2018) 419–430.
[54] X. Fei, W. Wei, Y. Tang, Y. Zhu, J. Luo, M. Chen, X. Liu, Simultaneous enhancements in toughness, tensile strength, and thermal properties of epoxy-anhydride thermosets with a carboxyl-terminated hyperbranched polyester, Eur. Polym. J. 90 (2017) 431–441.